

Present and future Stability of Larsen Ice Shelf (SOLIS)

GEF Loan 905 FINAL REPORT

Adrian Luckman, Daniela Jansen and Bernd Kulesa

Abstract

This report details initial findings for the second field season to the Larsen C ice shelf for NERC project SOLIS (2008-2011). Data collection was entirely successful and has yielded key findings regarding basal crevasses, that are currently under review in *The Cryosphere* journal. In addition, work is underway to interpret the signature of marine ice accreted at the base of the ice shelf which is clearly detected in a unique grid of GPR data collected near the ice shelf grounding line. GEF equipment played a vital role in generating these key datasets.

Background

In the wake of the successive disintegration of the northernmost part of the Larsen ice shelf (Larsen A) in 1995 and its southern neighbour (Larsen B) in 2002, the stability of the central (Larsen C; Figure 1) portion comes into question if the present warming trend continues. The -9° mean annual isotherm is considered the current limit of ice shelf viability on the Antarctic Peninsula and this isotherm is encroaching upon the northern reaches of the Larsen C ice shelf, which is by far the largest ($\sim 48600 \text{ km}^2$) ice shelf on the Antarctic Peninsula. Elucidation of the present and future stability of the Larsen C ice shelf is thus a current research priority challenging the scientific community

The SOLIS project ran from 2008 to September 2011 and its aim was to investigate the stability of the Larsen C ice shelf by a combined program of fieldwork, remote sensing and numerical modelling. A successful field season in 2008/09 was reported on in a previous GEF report (863, 864, 865). Funding was successfully sought for an additional field season, which required a further equipment loan consisting of a Pulse Ekko PE100 Pro GPR system and Leica 1200 differential GPS for geo-location. This report is for the second field season, which was as successful as the first.

Survey Procedure

Fieldwork was carried out during November and December 2009 by the author working through BAS logistics and aimed to investigate the structure of the ice shelf in a region near the Joerg peninsula (Fig. 1). The focus was on ice heterogeneity, shelf thickness and the signature of marine ice. Several hundreds of line kilometres of common-offset 50 MHz radar data were acquired using a system towed behind a snow-scooter (Figure 1b). Precise planimetric and height location of the antennas was recorded with a differential Leica System 1200 GPS. The GPR surveys were carried out with a sampling interval of 0.8 ns using 8 stacks. GPR traces were acquired every 3 s at a towing speed of approximately 5 km h⁻¹, yielding a trace spacing of ~ 4.3 m. Here we present parts of the GPR data that cover features of interest in the ice shelf. The second GPS receiver was left in camp to provide a differential reference, and was powered by solar panels and lead-acid batteries, which were also used to charge GPR and GPS batteries overnight.

Data quality

The quality of GPS data acquired was in excess of that required to locate the survey (~ 1 cm horizontal and ~ 2 cm vertical), but also served to provide ice surface profiles which aided the glaciological interpretation. The quality of GPR data was adequate for our purposes but the following should be noted:

- 1) Quality achieved was not as good as that of the previous field season which was loaned the newer GEF PE1000 system. The signal to noise ratio and consistence of signal amplitude were inferior.
- 2) As has been detailed in the initial report the GPR system suffered numerous hardware and operational problems. These included electrical connection problems, which required dismantling and resoldering of connections, and intermittent data capture failure (possibly related to weak cables) which required repeated stops to monitor progress in the field, and occasional re-survey where significant data was lost.

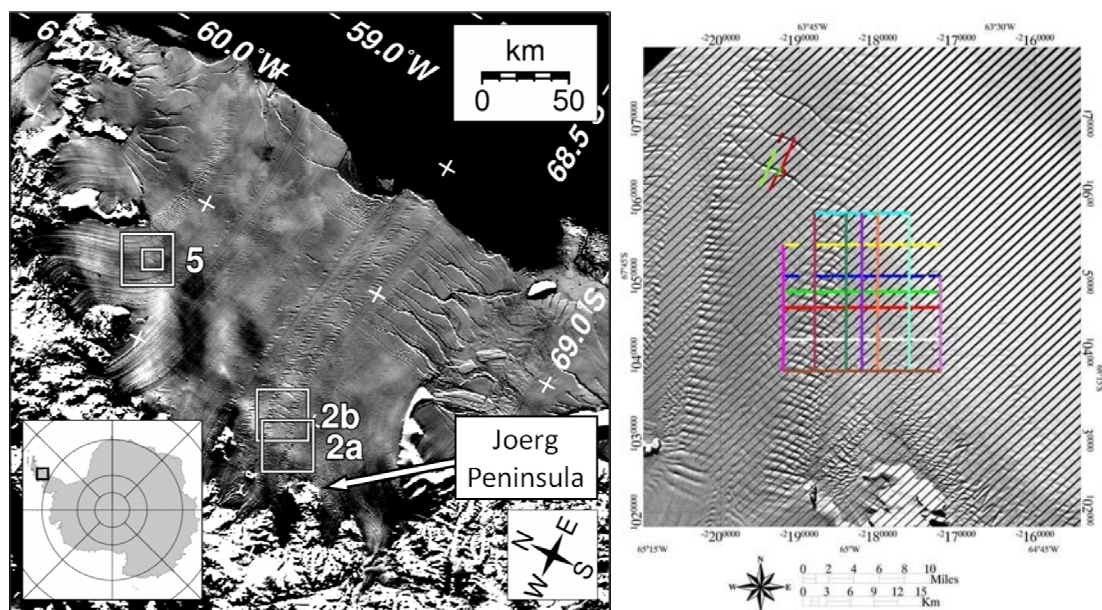


Figure 1. (a) Location of Larsen C Ice Shelf featuring an extract from MODIS MOA mosaic. Boxes indicate areas covered by later figures. (b) GPS records from successfully acquired GPR data in region labelled 2a and 2b.

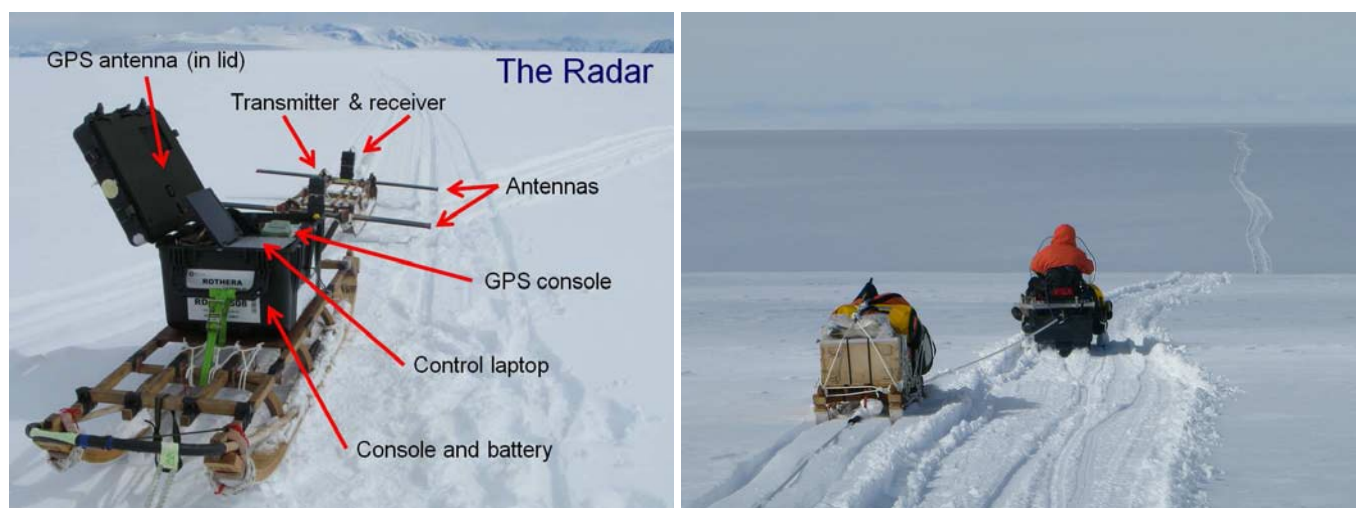


Figure 2. (a) GPR acquisition setup. Two sledges were towed behind a snow-scooter at around 5 km/hour. The first carried the GPS control box, laptop, GPS and lead-acid battery power, while the second, which had been stripped of all metallic parts, carried the transmitter, receiver and 50MHz antennas. (b) The radar-towing snowscooter was connected for safety reasons to a lead snowscooter, and some survey lines were repeated, as can be seen from the tracks in the snow.

Data Processing

GPS data were processed using standard Leica GeoOffice procedures. This was achieved overnight in the field to check for data completeness (including differential processing) and quality, and was repeated on return to the UK.

The raw GPR data were processed using standard techniques in Reflex-W including automatic gain control, band pass filtering, and correction for surface topography as recorded by dGPS. Again this was tested in the field to allow for adjustments of acquisition parameters, and then refined on return to the UK. Travel time was converted to depth assuming a radar-wave velocity in ice of 0.175 m ns^{-1} , a value based on fitting diffraction hyperbolae to data from a common mid-point (CMP) survey carried out

nearby on the same ice unit (not shown in this report). Trace positions were calculated precisely by linking the time signals associated with the GPR data to those of the GPS. Such a procedure was facilitated by making sure that the laptop clock was synchronised to GMT before surveys started, and timing was verified by comparing start and end times from field notebooks to those in the data files.

We present the data as un-migrated profiles because features deep in the ice column are more easily identified in printed figures by their characteristic hyperbolic returns.

Results

Analysis of data has focussed on two aspects of the science: Basal crevasses and marine ice accretions, the former of which has been the subject of a paper currently under review in *The Cryosphere* (Luckman et al., 2011).

Basal Crevasses

Figure 3 shows two series of features on Larsen C ice shelf (see Fig 1 for locations, labelled 2a and 2b). These are the surface expressions of basal crevasses that were investigated using the GPS profiles shown.

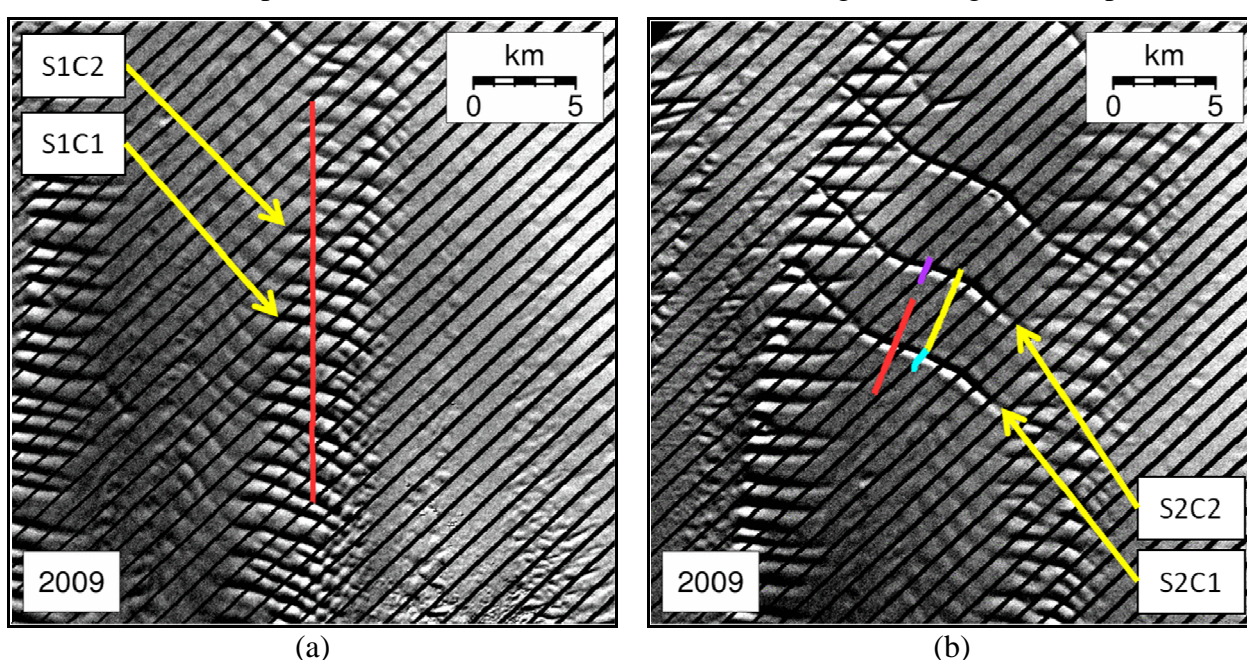


Figure 3. Landsat 7 sub-images from the southern end of Larsen C Ice Shelf showing features investigated in 2009 by RES along transects shown in various colours: (a) Series 1 of closely-spaced features; (b) Series 2 of widely-spaced features. See figure 1 for location within the ice shelf. Black diagonal stripes are due to a well-known Scan Line Correction fault.

Figures 4 and 5 show the processed radargrams from profiles over the two series of features. A single profile of GPR data was acquired from series 1, while from series 2, four profiles were acquired from and two from series 2. All radargrams collected from series 2 are presented to demonstrate the repeatability of the observations.

The key characteristics of basal crevasses in GPR data are the highly uneven basal return (in which the basal openings are usually evident), and the reflection from the crevasse tips (emphasized here by presenting un-migrated data). The crevasse tips are clearer for series 2 (Figs. 3b, 4) than for series 1 features (Figs. 3a, 4). Assuming the GPR profiles to be collected perpendicular to crevasses, the typical basal width of series 1 crevasses appears to be ~ 400 m, whilst for series 2, the complex basal echoes do not allow such an estimate to be made. The penetration height of series 1 crevasses is not as clear as series 2, but series 2 crevasses are chosen for further analysis as their crevasse tips are visible in the GPR data (Figure 5). Assuming that these echoes originate from the highest penetration point, the series 1 crevasse heights are around 100 m above the base of the ice shelf, which is close to one third of the ice shelf

thickness at this location. The penetration height of series 2 basal crevasses is between 180 m and 230 m above the base of the ice shelf, or around two-thirds of the ice thickness. In the absence of better error estimates from our own data, we assume that errors in basal crevasses penetration height are proportional to velocity errors from CMP surveys and are therefore $\sim 5\%$.

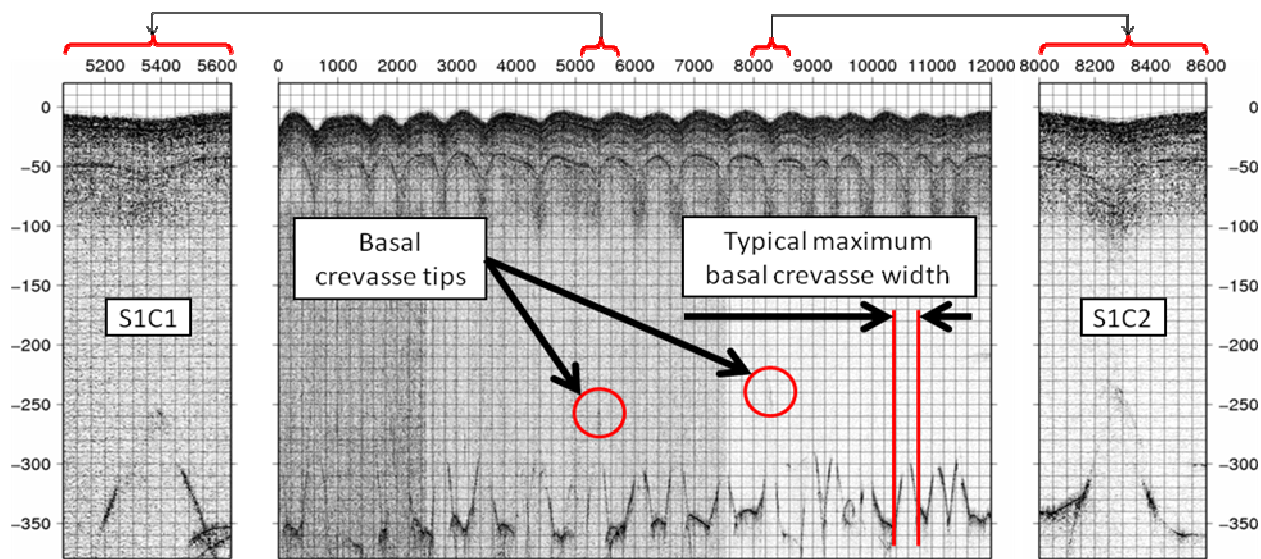
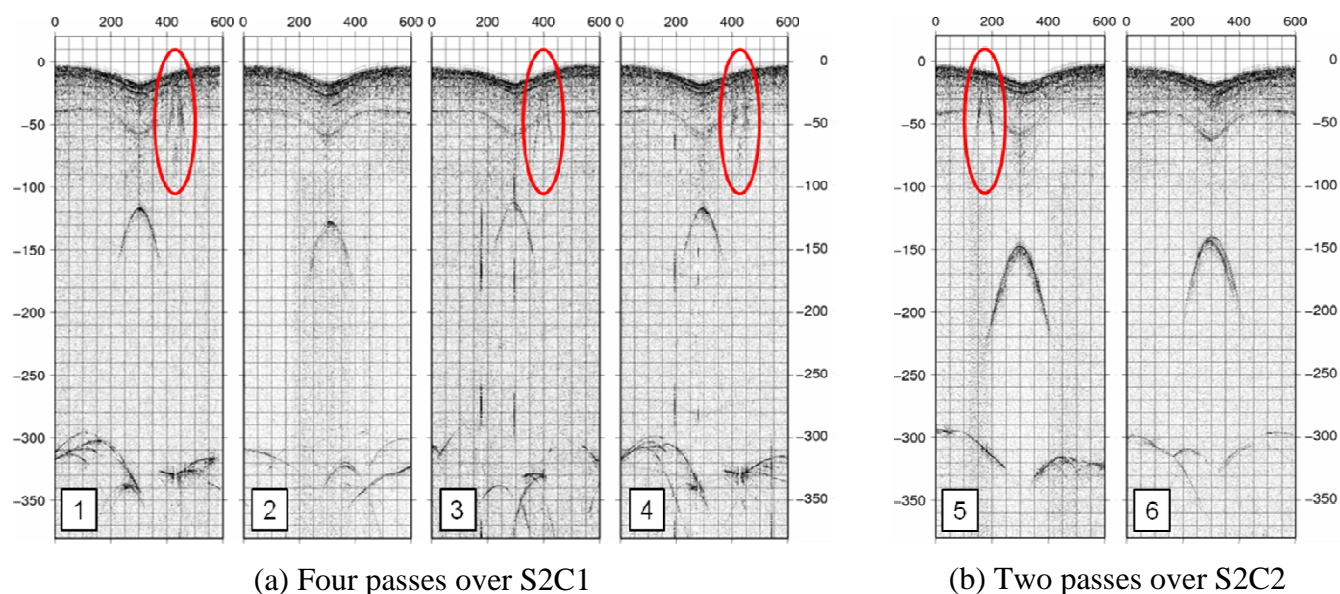


Figure 4. GPR data from Series 1 crevasses along the transect shown in Fig. 2a: Centre panel is the full 12 km profile, and right and left-hand panels show enlargement of S1C1 and S1C2 for clarity. Ice flow direction is left to right. Axes are in meters and not to scale: x-dimension assumes one radar pulse every 3 m of travel travel (for figure only - all measurements were made from data fully synchronised to the GPS signal) and y-dimension assumes a constant velocity in ice of 0.175 m/ns. Note the surface profile has been corrected using the dGPS data, showing the importance of this data acquisition to the interpretation.



(a) Four passes over S2C1

(b) Two passes over S2C2

Figure 5. Multiple GPR profiles over crevasses S2C1 and S2C2 along transects shown in Fig. 2b. Axes are in meters and not to scale: x-dimension assumes one radar trace every 4.3 m of travel travel (for figure only - all measurements were made from data fully synchronised to the GPS signal) and y-dimension assumes a constant velocity in ice of 0.175 m/ns. Multiple passes are illustrated to demonstrate measurement repeatability and correspond to coloured transects in Fig. 2b as follows; 1 and 4:blue, 2 and 3:red, 5:yellow and 6:purple. Flow direction in each case is left to right. Surface crevasse reflections highlighted in red. Surface profiles indicate the value of the dGPS data to understanding the impact of basal crevasses on the ice shelf structure and geometry.

In addition to the specific characteristics of the basal crevasses, two further aspects of the radargrams (Figs. 4 and 5) are of note. Firstly, hyperbolic radar responses originating near the surface, can be seen on the edges of some of the surface troughs and these are highlighted in Figure 5. Secondly, the ice shelf surface (as measured by dGPS) has troughs directly over each basal crevasse, and shallow internal layering within the ice follows approximately the profile of these surface troughs. Deeper layers, appear to be more deformed downwards above the basal crevasses than is the ice surface. For series 1 basal crevasses, the surface troughs are 5-10 m deep, and for series 2 they are ~10 m deep. The widths of these surface troughs are not well defined in either the GPS data or the satellite data as there is no clear break in slope. However, for both crevasse series the apparent surface deformation extends more than 500 m.

Marine ice accretion

In the first field season ground-penetrating radar (GPR) surveys were conducted to determine the detailed structure of the ice shelf at two control sites within and on either side of an inferred softer flow stripe on the southern Larsen C ice shelf, and to elucidate the ice mechanical properties at these sites. An anomalous reflector in about 100 m depth in the area of the flow stripe indicated that the different response to stresses within this feature might be due to the presence of marine ice. The slightly diffuse reflector might be interpreted as the base of a meteoric ice body, while seismic measurements yielded an ice shelf thickness of about 320 m, indicating the presence of marine ice in the lower ice column.

The second field season gave an opportunity to collect a 4 km GPR grid located on the same flow stripe further upstream, with the aim to get a three dimensional view of the boundary between meteoric and marine ice. Figure 6 shows a key part of that grid, and indicates preliminary findings with regard to the meteoric-marine ice boundary.

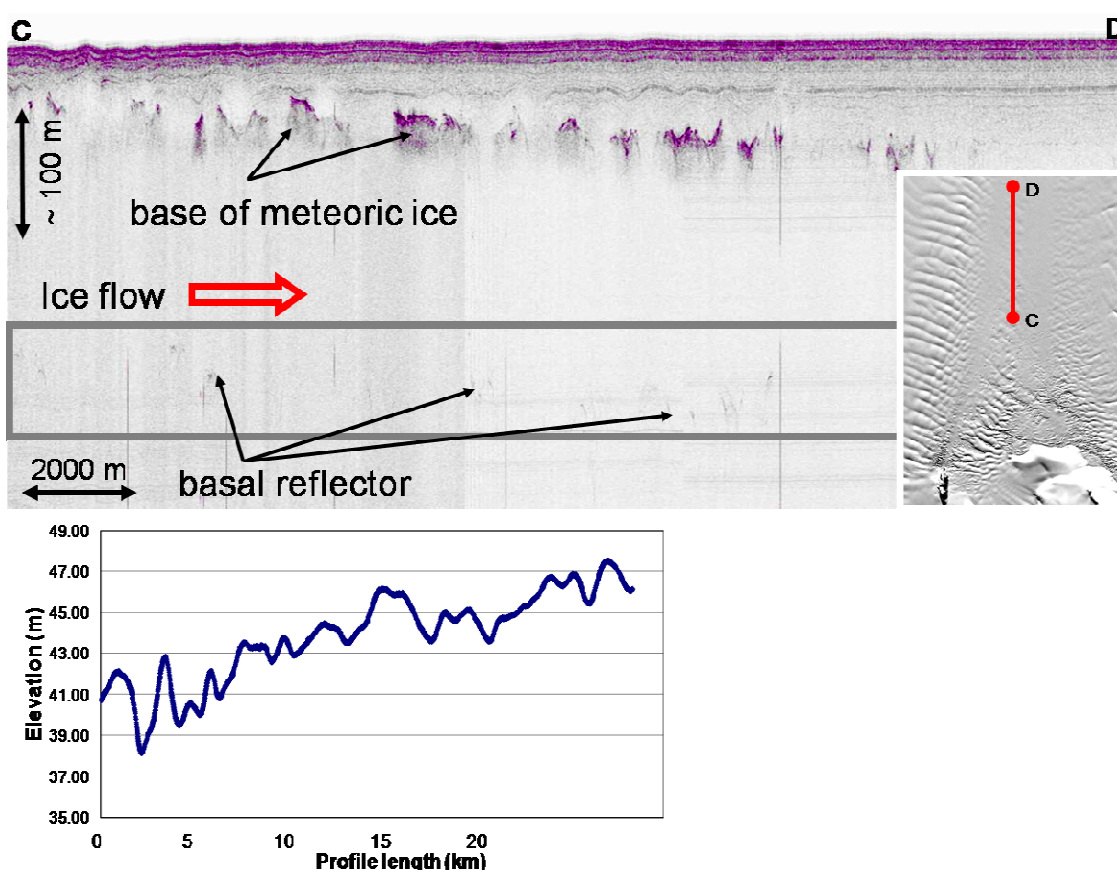


Figure 6: GPR Profile from the centre of the grid parallel to the ice flow direction. The reflector outlining the base of the meteoric ice is dipping due to the accumulation of snow during advection downstream. The profile cuts across the meteoric ice blocks coming from the small glacier on the Jörg Peninsula. The GPS elevation data show an increase in flow direction, indicating ongoing accretion of marine ice.

The reflector is clearly visible within all profiles crossing the flow stripe and is dipping towards flow direction, reflecting accumulation at the ice shelf surface. No seismic survey was conducted in the second field season, but the GPS elevation data indicates that marine ice must be present in the lower part of the ice column to reach hydrostatical equilibrium. Figure 7 shows a transverse profile over the marine ice band and illustrates the complex nature of the ice shelf in this region. The decreasing surface elevation towards the centre of the profile is not sufficient to explain a change in ice thickness as high as seen in the radar data, suggesting that a layer of marine ice, which cannot be penetrated by the radar, has accreted underneath the thin meteoric ice. We assumed marine ice to have a density of 920 kg/m^3 (fully consolidated ice without air inclusions), sea water to have a density of 1028 kg/m^3 . The density of meteoric ice was calculated from the seismic measurements made during the first field season, and is dependent on depth (Jansen et al., 2010).

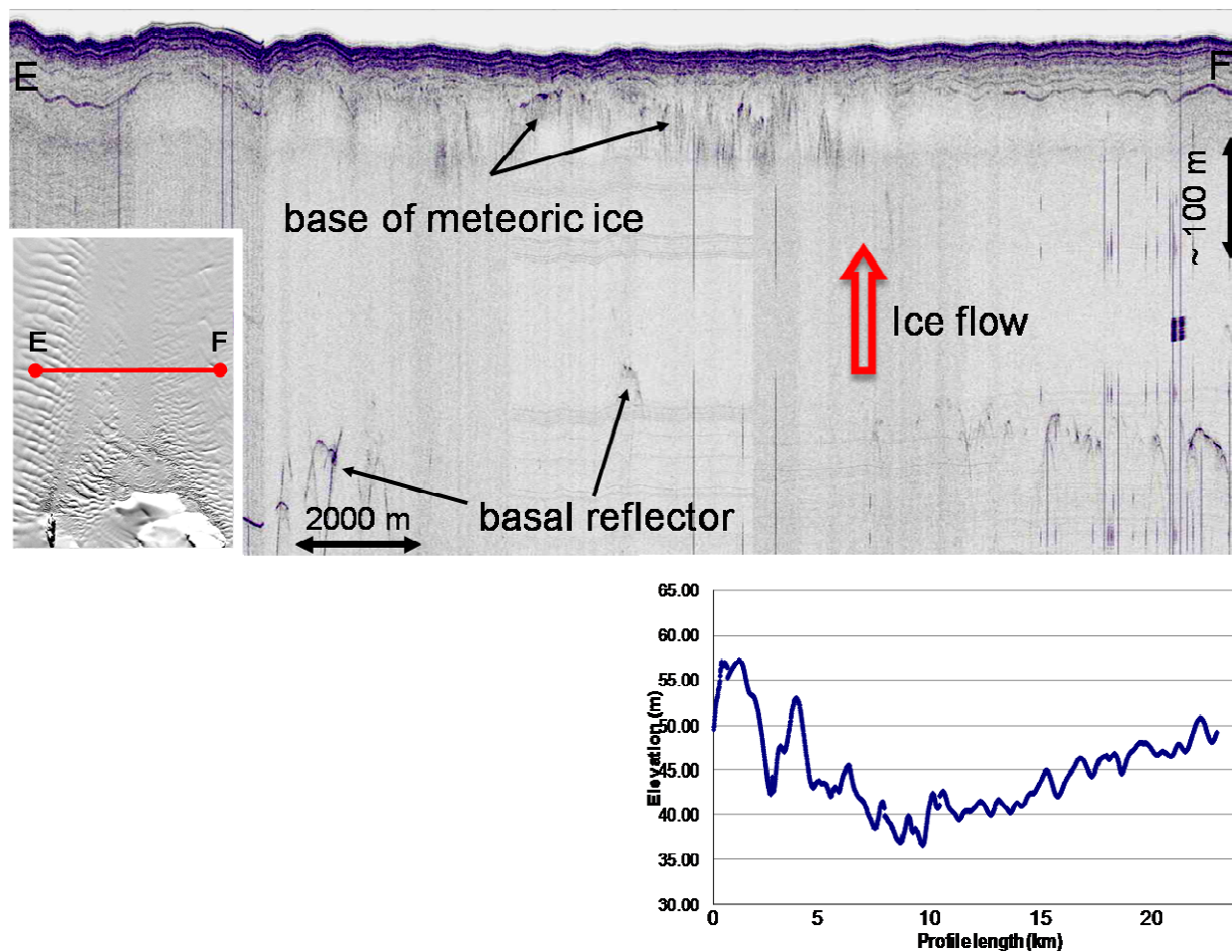


Figure 7: GPR Profile cutting across the flow band and the two adjacent ice shelf units. On the left the GPS profile reflects the topography of the basal crevasse features show in figure 3b. The transition between meteoric ice bands and the flow feature with the accreted marine basal ice layer is clearly visible, as well as the meteoric ice blocks in the centre of the suture zone. The relative change in elevation along this profile shows that the diffuse reflector cannot be the base of the ice shelf and that there has to be a marine ice layer underneath to maintain hydrostatic equilibrium. Cross profiles further downstream show a less relative change towards the centre of the profile. This might be interpreted as ongoing accretion of marine ice as the reflectors in the upper layers indicate equal accumulation rates in the area of the suture zone and the adjacent ice shelf units.

Conclusion and Recommendations

The quality and scope of data acquired during the second SOLIS field season justifies the extra resources that were given to the project. Using these data we have already highlighted the potential importance of

basal crevasses to ice shelf interactions with the ocean and potential stability. Work will continue to better understand the role of marine ice in ice shelf mechanics, and to quantify the rate at which it is accreted to the base of the ice shelf.

We have demonstrated that snow-scooter towed GPR can adequately quantify key ice shelf structural features. We recommend that all similar future studies incorporate dGPS acquisition, as the surface profile is vital in elucidating the structure of the ice shelf below.

Publications

A. Luckman, D. Jansen, B. Kulessa, E. C. King, P. Sammonds, and D. I. Benn, 2011, Basal crevasses in Larsen C Ice Shelf and implications for their global abundance, *The Cryosphere Discuss.*, 5, 2035-2060, 2011

This work has also been presented at:

1. Antarctic Peninsula Climate Change Workshop, Leeds, June 2010
2. NERC AFI workshop, Cambridge, September 2010
3. EGU 2010: Geophysical Research Abstracts Vol.12, EGU2010-10869,2010
4. EGU 2011: Geophysical Research Abstract Vol.13, EGU2011-12917, 2011
5. FRISP (Forum for Research into Ice shelf Processes) Workshop, Bad Bererkesa, Germany, June 2010

Acknowledgements

Without the excellent equipment and service provided by the GEF, this project would not have been possible. We thank the staff for their swift response to problems, and for their understanding when the equipment was returned with water damage that occurred during the return transit. Fieldwork and Daniela Jansen were funded by NERC through the Antarctic Funding Initiative (AFI) (NE/E012914/1).

References

Jansen, D., Kulessa, B., Sammonds, P. R., Luckman, A., King, E. C., Glasser, N. F., Oct. 2010. Present stability of the Larsen C ice shelf, Antarctic Peninsula. *Journal of Glaciology*, 593-600.